A mixed disulfide bond in bacterial glutathione transferase: Functional and evolutionary implications

ARTICLE *in* STRUCTURE · JULY 1998

Impact Factor: 5.62 · DOI: 10.1016/S0969-2126(98)00074-4 · Source: PubMed

A mixed disulfide bond in bacterial glutathione transferase: functional and evolutionary implications

Jamie Rossjohn[1], Galina Polekhina[1], Susanne C Feil[1], Nerino Allocati[2], Michele Masulli[2], Carmine Di Ilio[2] and Michael W Parker[1]*

Background: Glutathione *S*-transferases (GSTs) are a multifunctional group of enzymes, widely distributed in aerobic organisms, that have a critical role in the cellular detoxification process. Unlike their mammalian counterparts, bacterial GSTs often catalyze quite specific reactions, suggesting that their roles in bacteria might be different. The GST from *Proteus mirabilis* (PmGST B1-1) is known to bind certain antibiotics tightly and reduce the antimicrobial activity of β-lactam drugs. Hence, bacterial GSTs may play a part in bacterial resistance towards antibiotics and are the subject of intense interest.

Results: Here we present the structure of a bacterial GST, PmGST B1-1, which has been determined from two different crystal forms. The enzyme adopts the canonical GST fold although it shares less than 20% sequence identity with GSTs from higher organisms. The most surprising aspect of the structure is the observation that the substrate, glutathione, is covalently bound to Cys10 of the enzyme. In addition, the highly structurally conserved N-terminal domain is found to have an additional β strand.

Conclusions: The crystal structure of PmGST B1-1 has highlighted the importance of a cysteine residue in the catalytic cycle. Sequence analyses suggest that a number of other GSTs share this property, leading us to propose a new class of GSTs – the beta class. The data suggest that the *in vivo* role of the beta class GSTs could be as metabolic or redox enzymes rather than conjugating enzymes. Compelling evidence is presented that the theta class of GSTs evolved from an ancestral member of the thioredoxin superfamily.

Addresses: [1]The Ian Potter Foundation Protein Crystallography Laboratory, St Vincent's Institute of Medical Research, 41 Victoria Parade, Fitzroy, Victoria 3065, Australia and [2]Dipartimento di Scienze Biomediche, Università 'G. D'Annunzio' di Chieti, Via dei Vestini 31, 66013 Chieti, Italy.

*Corresponding author.
E-mail: mwp@rubens.its.unimelb.edu.au

Key words: cysteine chemistry, evolution, glutathione transferase, thioredoxin, X-ray crystallography

Received: **2 February 1998**
Revisions requested: **19 March 1998**
Revisions received: **30 March 1998**
Accepted: **7 April 1998**

Structure 15 June 1998, **6**:721–734
http://biomednet.com/elecref/0969212600600721

Introduction

Glutathione *S*-transferases (GSTs; EC 2.5.1.18) are a multifunctional superfamily of enzymes that play a vital role in the cellular detoxification process. They achieve this by conjugating the tripeptide glutathione (GSH) to a wide range of endobiotic and xenobiotic electrophilic substrates. As a direct consequence of their role in detoxification, GSTs have been implicated in the development of the resistance of cells and organisms towards drugs, insecticides, herbicides and antibiotics [1,2].

Cytosolic GSTs exist as dimers with a subunit molecular weight of about 25 kDa and have been grouped into at least seven distinct classes — alpha, kappa, mu, pi, sigma, theta and zeta — on the basis of substrate specificity and primary structure [3–7]. Generally, the intraclass amino acid sequence identity is greater than 70%, whereas the interclass identity is usually less than 30%. The theta class GSTs have been proposed as the evolutionary forerunner of the other classes on the basis of the apparent distribution of the former in a diverse range of organisms including bacteria, yeast, plants and insects [8,9]. Crystal structures from the alpha, mu, pi, sigma and theta class complexed with various inhibitors and substrates have been reported (for reviews, see [10–12]). These studies have shown that the overall polypeptide fold is similar: the N-terminal domain consists of a central core of mixed four-stranded β sheet surrounded on one side by a pair of α helices and on the other by another helix and irregular structure, whereas the C-terminal domain is all α helical. Each class exhibits unique features, especially around the active site and the C terminus, that define the substrate repertoire for a particular GST. The active site actually consists of two binding sites: the G site where GSH binds and the H site where hydrophobic electrophiles bind. A tyrosine residue near the N terminus was observed to hydrogen bond onto the sulfur atom of GSH in the alpha, mu, pi and sigma class crystal structures. Mutagenesis studies have confirmed that this tyrosine is responsible for the activation of GSH by promoting thiolate formation (for reviews, see [10–12]). In contrast, a serine residue near the N terminus has replaced the role of the tyrosine in theta-class enzymes [13–15].

GSTs have only recently been discovered in bacteria and hence little is known about their properties. They have

been detected in *Escherichia*, *Proteus*, *Pseudomonas*, *Klebsiella*, *Enterobacter* and *Serratia* species [16–18]. A number of bacterial GSTs possess highly specific activities: dichloromethane dehalogenase [19], tetrachlorohydroquinone dehalogenase [20], stringent starvation protein [21] and a β-etherase [22]. One of the best characterised bacterial GSTs is one from *Proteus mirabilis* (PmGST B1-1, where B denotes its bacterial origins and 1-1 denotes it is a homodimer) [16]. This enzyme displays distinct kinetic and immunological properties compared with mammalian GSTs and exhibits either minimal or no detectable activity towards a range of standard GST substrates. PmGST B1-1 shares high sequence identity with a number of other bacterial GSTs but possesses less than 20% sequence identity with alpha, mu, pi and sigma class GSTs [11,23]. The enzyme has been classified as a theta class GST on the basis of limited sequence identity with its mammalian counterpart [4,8,24].

PmGST B1-1 is particularly interesting as it can bind to a range of antibiotics and reduce the antimicrobial activity of β-lactam drugs [25,26]. A structural understanding of antibiotic interaction with bacterial GSTs may prove useful in treating bacterial resistance towards antibiotics. Another intriguing feature of PmGST B1-1 concerns its catalytic mechanism. Its current classification as a theta class GST suggests that Ser9 should be involved in stabilization of the thiolate form of GSH. However, mutagenesis studies of this residue and all other likely candidate residues in the N-terminal domain have failed to identify which residue is taking the role of the catalytic tyrosine or serine observed in the other GST classes.

We have determined the structure of PmGST B1-1 from two different crystal forms. Surprisingly, the thiol group of GSH is found covalently bound to Cys10. In the reduced state, there are a number of candidates likely to fulfil the role of stabilizing the thiolate form of GSH: these include the mainchain amide of Cys10 or His106 from the C-terminal domain. The observation of the mixed disulfide prompted us to re-evaluate the functional role of PmGST B1-1 and its classification as a theta class GST, leading to the proposal that it belongs to a novel GST class we term beta. Furthermore, we have revisited the proposal that GSTs may have evolved from a thioredoxin-like ancestor [27–29] and present new data that provide compelling support for the case of divergent evolution of the two superfamilies.

Figure 1

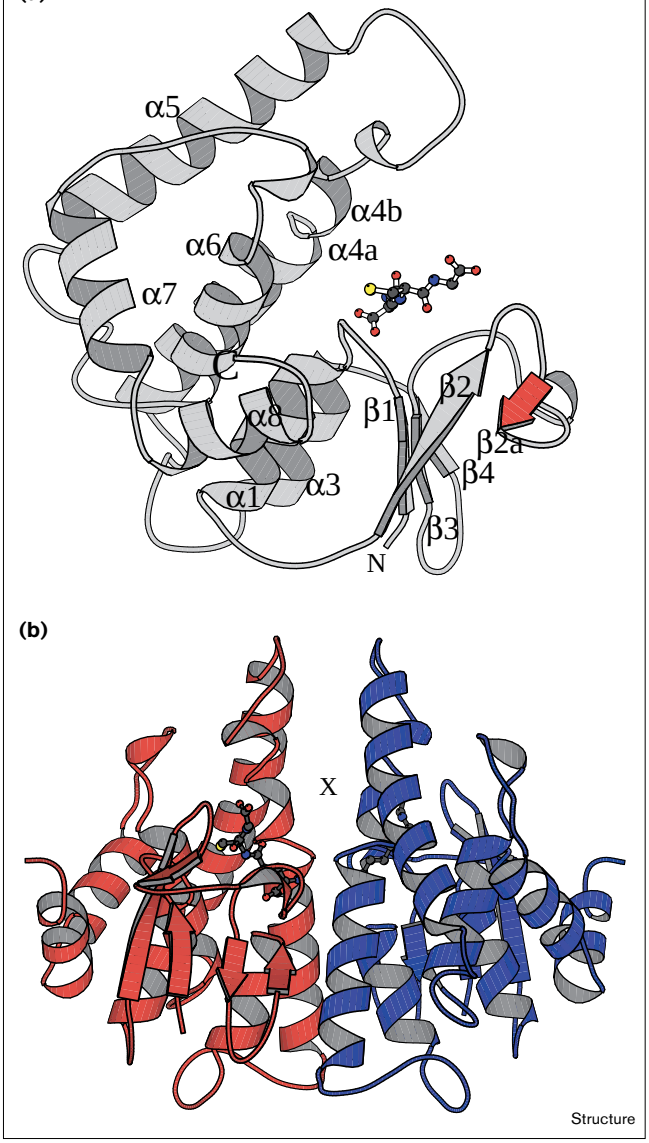

Schematic representation of PmGST B1-1. **(a)** The monomer with bound GSH. The extra β strand (see text) is highlighted in red. **(b)** The dimer. The location of the hydrophobic cavity in the interface is marked by X. The GSH molecules are also indicated in ball-and-stick representation. (These figures were generated using the program MOLSCRIPT [56].)

Results

The protein fold

The crystal structure of PmGST B1-1 has been determined in two different crystal forms. In crystal form I, there is a monomer in the asymmetric unit (so that the physiological dimer is generated by a noncrystallographic twofold axis), whereas in crystal form II there are two dimers. The structures of all three dimers are essentially identical. The rms deviation of Cα positions on superposition is 0.30 Å with no deviations greater than 1.0 Å.

PmGST B1-1 is a homodimer of two identical subunits with each monomer containing 203 amino acids, although we only see density for residues 1–201 in both structures. The monomer comprises two domains (Figure 1a). The N-terminal domain (residues 1–74) contains a βαβ unit

Figure 2

Stereoview of the dimer contacts of PmGST B1-1 looking perpendicular to the molecular twofold axis. Monomers A and B are shown in blue and red, respectively. (The figure was generated using the program MOLSCRIPT [56].)

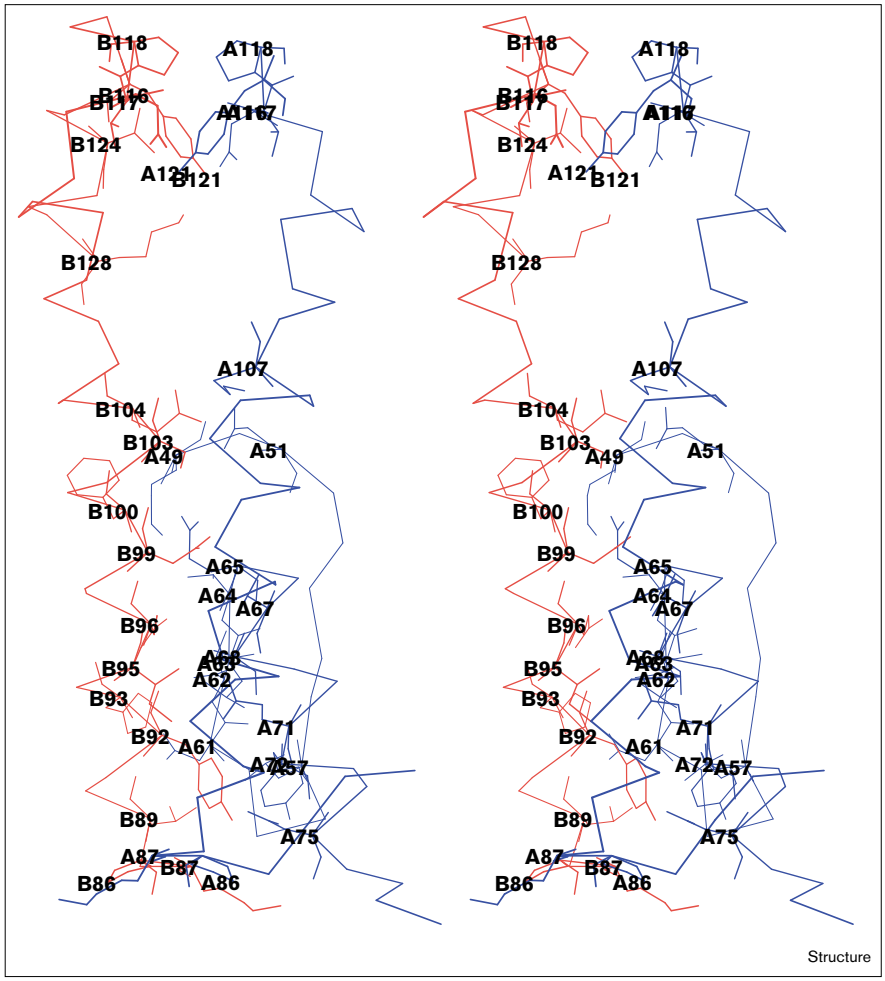

(residues 1–31) connected to a ββα unit (residues 54–74) via a long surface-exposed region. This region contains a small β strand (β2α; residues 36–37) followed by one turn of a 3_{10} helix (α2; residues 43–45). (The secondary structure nomenclature has been made consistent with other published GST structures.) The observation of the β strand in this region was surprising, as none of the other published GST crystal structures have this strand. Thus, unlike the other GSTs, PmGST B1-1 has a five-stranded mixed sheet in the N-terminal domain. A 14-residue linker connects this domain to the mostly α-helical C-terminal domain. The latter domain (α8; residues 89–201) contains five α helices and ends in a small C-terminal helix (residues 189–196) and a short coil (residues 196–201). Helix α4 is more accurately described as two helices: α4A (residues 89–103) and α4B (residues 106–109) followed by a turn of 3_{10} helix (residues 111–113).

The dimer has approximate globular dimensions of 60 Å × 65 Å × 50 Å (Figure 1b). In contrast to all other GST structures, there is no V-shaped dimer interface. The dimerization contacts are located both at the base of the molecule and further up the helical towers of the interface (Figures 1b and 2). The contacts observed near the top of the helical towers have not previously been observed in other GST structures and are caused by intersubunit rotations. Most of the interactions at the subunit interface are polar in character. There are five hydrogen bonds (Gln51–Glu104, Asp61–His93, Thr64–Glu96, Glu65–Asn99 and Asp75–Tyr72) and no salt bridges at the base. In addition, there is a hydrophobic interaction between Tyr72 and its symmetry mate and with Leu57 and Leu89 of the other monomer. Approaching the top of the towers is another aromatic–aromatic interaction (between Tyr121 and its symmetry mate) in addition to two salt bridges (Glu104–Lys107 and Asp116–Lys128).

The GSH-binding site (G site)

The GSH molecule is bound in an extended fashion in the G site with the γ-glutamyl moiety pointing towards the core

of the molecule and the glycyl moiety pointing towards strand β2a (Figures 1, 3 and 4). This mode of binding is consistent with the observed binding found in other GSTs (for reviews, see [10–12]). The interactions are a mixture of hydrophobic and polar links together with one salt bridge and a covalent bond (Figure 4). The γ-glutamyl moiety is strongly tethered to the protein with eight of the 11 polar interactions seen between the protein and GSH. There are three interactions with the other monomer: Asn 99, Ser 103 and Glu104. The latter interaction is also seen in the alpha [28], mu [30], pi [27,31] and sigma [32] classes but not in the insect [13] and plant [33] theta class GSTs. Glu65 is in the generously allowed region of the Ramachandran plot and the strained stereochemistry is presumably counteracted by binding to GSH. The equivalent residue in other GST structures also adopts a strained conformation [13,27,28,30–33]. The interaction of His106 and Lys107, residues from the C-terminal domain, with substrate is of interest as only residues in the N-terminal domain or from the C-terminal domain of the other monomer have previously been observed to interact with GSH. A novel feature of the binding is the observation that the sulfur atom of the cysteinyl moiety is covalently bound to Cys10. The glycyl moiety of GSH only forms one polar interaction, a salt bridge, with the protein and so appears less firmly bound to the protein in comparison to the γ-glutamyl and cysteinyl moieties. There are, however, three van der Waals interactions (Ser9, Leu32 and Gln51) that serve to stabilize it. Unlike the mu, pi, sigma and theta class GSTs, PmGST B1-1 does not contain a conserved aromatic residue from the region between strands β2 and β3 that interacts with GSH. There is one *cis*-proline in the structure (Pro53) and it is located in a β turn that lines the G site. This *cis*-proline is conserved in all GST structures and appears to be critical for ensuring mainchain hydrogen bonding about this region to the cysteinyl moiety of the GSH substrate [13,27,28,30–33].

The binding site for hydrophobic electrophiles (H site)

One distinctive feature of GSTs is their ability to bind to a wide range of substrates. This diversity, in part, arises from the low sequence identity and hence structural heterogeneity within the C-terminal domain which contributes many of the residues to the H site [13,28,30–33]. The H site in PmGST B1-1 is principally made up of aromatic residues: His167, Phe113 and Trp164. There is also a polar aliphatic residue lining the H site, Ser110. A glycine residue (Gly8) is located at the base of the site. Unlike most other GSTs, the H site here is very open and more polar and the C-terminal tail does not encroach into the site.

Discussion

Comparison to other GST structures

PmGST B1-1 shares less than 20% sequence identity with the alpha, mu, pi and sigma class GSTs. Despite this low sequence identity, PmGST B1-1 adopts a similar three-dimensional fold to the other GST classes for which structures are known. In particular, the N-terminal domain is very similar with rms superpositions of Cα atoms between GST classes ranging between 1.4 and 1.8 Å. The C-terminal domain is less similar, with differences in the length, curvature and orientation of the helices. One of the biggest differences between the bacterial GST and GSTs of the other classes is a large subunit rotation of between 19° and 33° required to superimpose dimers. The published theta class GST crystal structures have been extensively compared with published mammalian GST crystal structures elsewhere [13,33] and hence a detailed comparison will not be repeated here.

The crystal structures of two theta class GSTs, from an insect and a plant, have recently been determined [13,33]. The level of sequence identity between PmGST B1-1 and the theta class enzymes is low (25% for both).

Figure 3

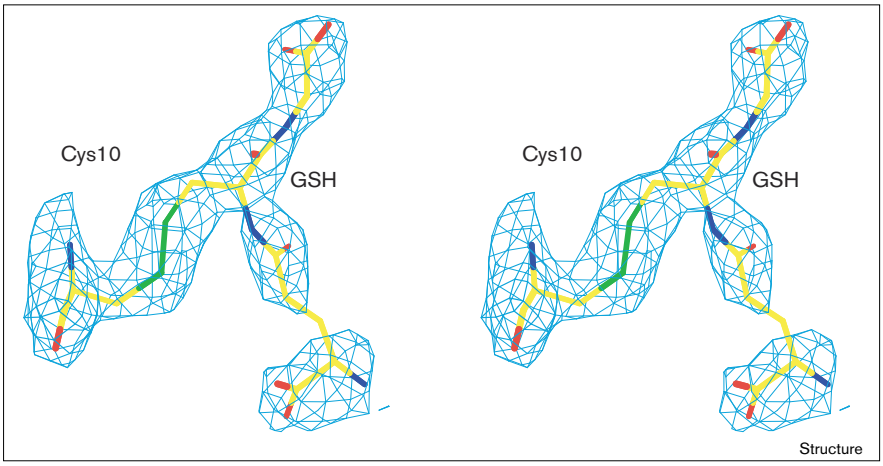

Stereo view of the $2F_{obs}–F_{calc}$ electron-density map showing the density for the mixed disulfide bond in the active site of PmGST B1-1. The data are from the GSH complex of crystal form II. The map is a simulated annealing omit map where the substrate and all neigboring residues were removed before refinement and map calculation. The contour level is 1σ.

Figure 4

Schematic figure illustrating the residues contacting the substrate GSH. (The figure was generated using the program LIGPLOT [57].)

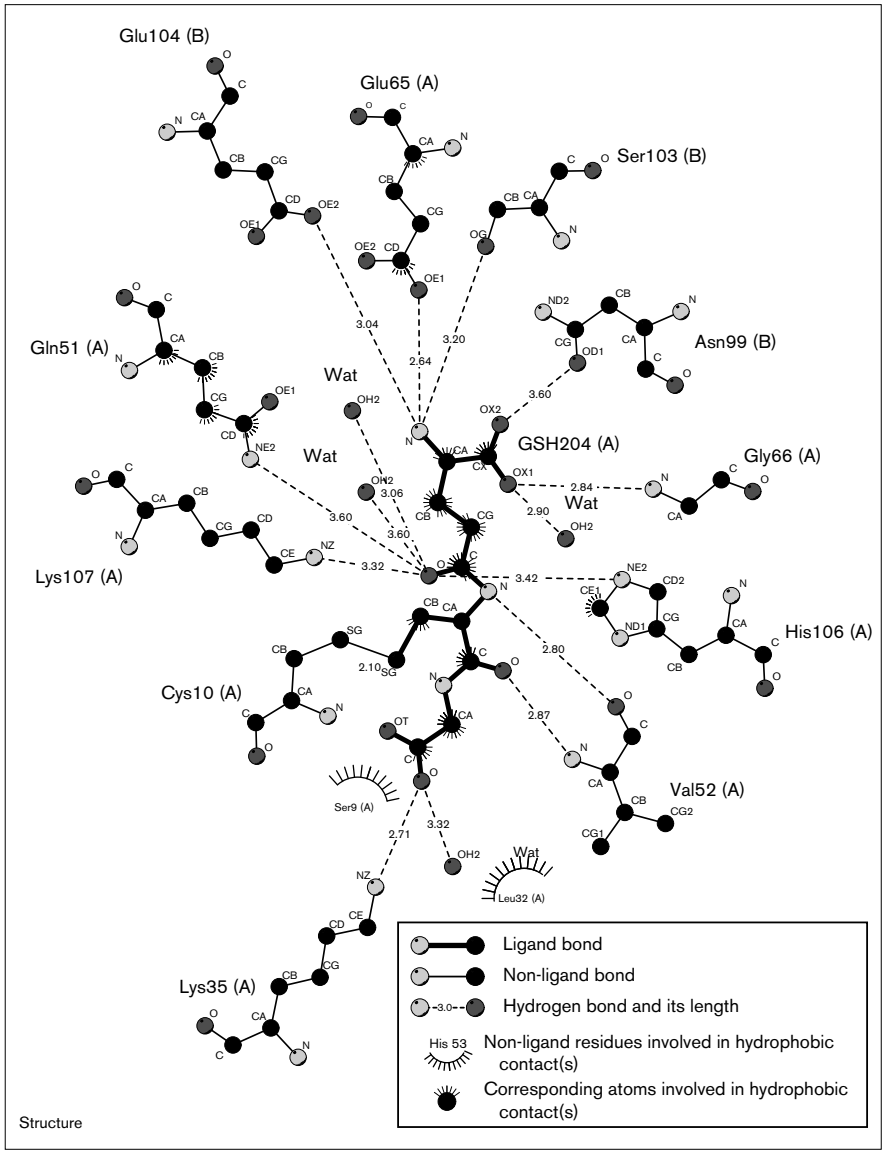

However, the overall rms deviation on superposition of the crystal structures is 1.53 Å (for 162 Cα atoms) between PmGST B1-1 and insect GST and 1.80 Å (for 156 Cα atoms) between PmGST B1-1 and plant GST, reflecting closely similar overall structures (Figure 5). The N-terminal domain of PmGST B1-1 shares a sequence identity of 30% with the insect GST and 33% with the plant GST whereas the identities for the C-terminal domain are only 21% and 16%, respectively.

One of the most striking differences between the structures is the close-packed dimer interface, dominated by polar interactions, in the bacterial enzyme in contrast to the more open, V-shaped, interface dominated by hydrophobic interactions in the other two structures. An intersubunit 'lock-and-key' hydrophobic interaction has been described in the mammalian GST structures [30]. This involves an aromatic residue (Phe52 in alpha, Phe56 in mu and Tyr49 in pi), termed the 'key', from the loop preceding strand β3 and a hydrophobic 'lock' from the helices α4 and α5 of the other monomer. However, in the sigma class GST there is no lock or key and the interface is dominated by polar rather than hydrophobic interactions [32]. It has been argued that the squid gene diverged from either a theta or an alpha/mu/pi precursor which originally encoded a protein that lacked the lock and key for subunit dimerization. The theta-class enzymes, however, have subsequently been found to share some of the subunit interface traits of the alpha, mu and pi enzymes. The plant GST possesses the hydrophobic key residue (Phe49) but in the insect enzyme

Figure 5

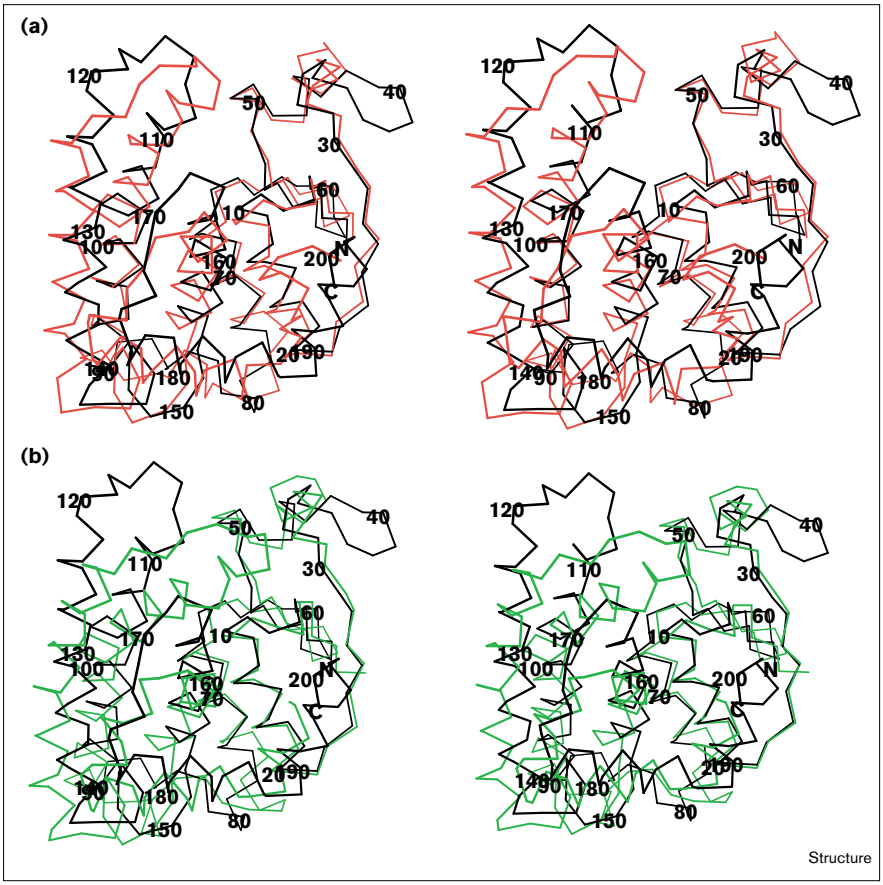

Comparisons of theta class enzymes. Stereoview Cα trace of the superposed bacterial GST (black trace) with **(a)** insect GST (red trace) [13] and **(b)** plant GST (green trace) [33]. The superpositions are based only on the N-terminal domains of each protein. (The figure was generated using the program MOLSCRIPT [56].)

a key from the C-terminal domain (Phe140) is employed. In contrast, the bacterial enzyme has a predominantly polar interface and no lock or key. Although the interfaces of both sigma and bacterial GSTs are polar, the specific interactions are largely different: the Thr64–Glu96 interaction seen in the bacterial enzyme is the only conserved interaction (Ser61–Glu89 in the sigma class GST). Another difference in the interface concerns the unusual packing of symmetry-equivalent arginine residues observed in the alpha, mu, pi and sigma classes [28,30–32]. No corresponding interaction is seen in either the bacterial, insect or plant GST structures [13,33].

Despite all these differences, there are marked similarities between the structures. All three have truncated C-terminal extensions and very open H sites. In the N-terminal domain there are 12 strictly conserved residues: Pro7, Ser9, Leu32, Phe43, Leu44, Asn47, Pro48, Pro53, Glu65, Ala68, Ile69 and Tyr72. Four of these residues (Ser9, Leu32, Pro53 and Glu65) are ligands for GSH. However, only PmGST B1-1 has G site ligands (Asn99, Ser103 and Glu104) contributed from the neighbouring monomer. Asn47 is a conserved residue amongst the theta class GSTs [34]: in the bacterial, insect and plant GST structures it appears to have a critical role in stabilizing the loop before the functionally important *cis*-proline. Part of the loop (residues 42–48 in PmGST B1-1) between strands β2 and β3, a highly flexible and conformationally variable region in GST structures [10,11], adopts a very similar conformation in the bacterial, insect and plant enzymes. This region does not exhibit higher than average temperature factors in PmGST B1-1 or, for that matter, in other theta class GSTs [13,33]. A possible reason for similar conformations and lower flexibility is the presence of a conserved aromatic residue (Phe43 in bacterial GST, Phe43 in insect and Phe45 in plant) in this region which is positioned in a mostly conserved hydrophobic pocket made up of residues from the β sheet in the N-terminal domain. In particular, there is a stacking interaction formed between this residue and a conserved aromatic residue (Tyr4 in bacterial GST, Tyr4 in insect and Phe6 in plant). There are six strictly conserved residues in the C-terminal domain: Lys128, Leu140, Gly148, Thr152, Asp155 and Ala183. The biggest difference in this domain is the helix α4–loop–helix α5 region which has a highly pronounced curvature in the plant enzyme (Figure 5).

Figure 6

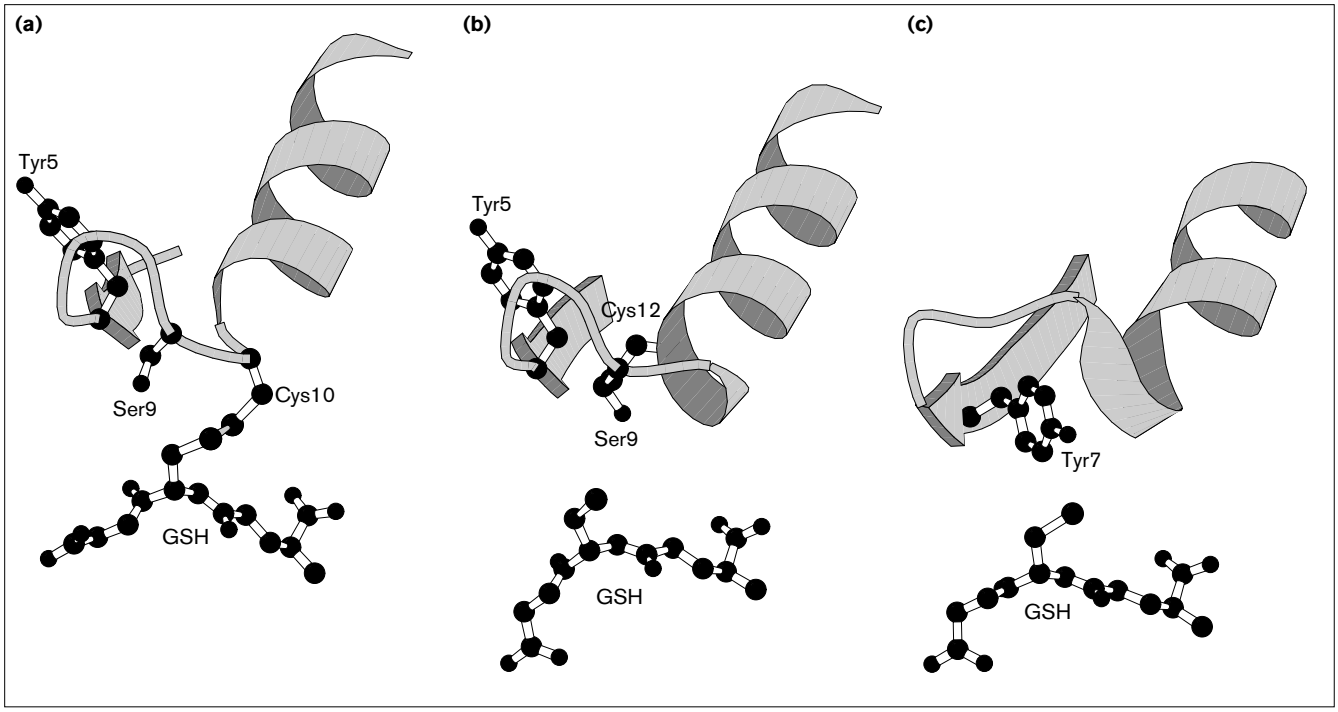

Evolution of GSH thiol interactions within the active sites of different GSTs. The active sites of GSTs from three classes are shown: **(a)** bacterial theta class GST **(b)** insect theta class GST [13]; and **(c)** human pi class GST [31]. GSH and residues involved in the interactions are shown in ball-and-stick form. (The figure was produced using MOLSCRIPT [56] and is adapted from Figure 5 of [12] ©1997 American Chemical Society with kind permission of Richard Armstrong.)

The conserved catalytic tyrosine found in the alpha, mu, pi and sigma classes and the conserved catalytic serine residue in the theta class are retained in position 5 and 9, respectively, in PmGST B1-1 (Figure 6). Tyr5 points away from the active site whereas Ser9 is within hydrogen-bonding distance of the GSH thiol. Unlike the other classes, the GSH thiol is covalently bound to the sulfur atom of Cys10 in the bacterial enzyme (Figures 3, 4 and 6).

The antibiotic-binding site

Binding of antibiotics to PmGST B1-1 has been monitored by tryptophan fluorescence [25], suggesting the location of at least one tryptophan residue close to the antibiotic-binding site. On the basis of crystallographic studies of GST complexes, there are two likely sites where antibiotics might bind to the enzyme — in the H site or in the dimer interface. An antischistosomal drug has been shown to bind in the dimer interface of schistosomal GST [35] and a GSH conjugate was observed to bind in the interface of a squid GST [32]. Superposition of these structures with PmGST B1-1 indicates that both sites are occluded in the bacterial enzyme. There is, however, a hydrophobic cavity large enough to bind an antibiotic molecule located between these two sites at the dimer interface (see Figure 1b). This site is lined by the residues Gly108, Ser110, Pro111 and the aliphatic sidechain portions of residues Lys107, Lys128 and Lys132. There is a tryptophan residue, Trp164, approximately 15 Å away from the centre of the cavity. As this same tryptophan lines the H site, it is not possible to exclude either site as the antibiotic-binding site on the basis of the fluorescence measurements. However, because antibiotics bind to the enzyme in a non-competitive manner with respect to the classical GST substrate 1-chloro-2,4-dinitrobenzene (CDNB), it is likely that the antibiotic-binding site is located at the dimer interface as CDNB binds in the H site [26].

The active site and catalytic mechanism

One of the most significant findings in this study is the observation that the GSH thiol is covalently bound to the sulfur atom of Cys10. Simulated annealing omit maps in this region for both crystal forms clearly indicated the covalent linkage (Figure 3). The presence of the mixed disulfide in solution has been confirmed by mass spectrometry. The difference in molecular mass of 336 Da between wild-type enzyme and a Cys10→Ala mutant in solution is compatible with the mutation and the presence of one GSH molecule per monomer (E Casalone, I Ceccarelli, NA, MM, G Federici and CDI, unpublished results). The finding of a mixed disulfide is a surprising result in

two regards. Firstly, involvement of a cysteine in the catalytic mechanism of GSTs has not previously been documented. The thiolate form of GSH has been shown to be involved in the catalytic mechanism of other GSTs and is stabilized by interactions with a tyrosine residue near the N terminus in the alpha, mu, sigma and pi classes [27,28,30–32] or by a serine/threonine residue near the N terminus in the theta class enzymes [13–15]. Secondly, there is the puzzle as to how the GSH thiol can react with substrates if it is covalently bound to the protein.

Clearly, for the bacterial GST to perform a conjugating reaction with GSH, the disulfide bond between GSH and Cys10 must either not be formed or must be broken in the catalytic mechanism. As PmGST B1-1 is predominantly located in the periplasm [36], where a number of proteins are located that can catalyze the break-up of disulfide bonds, it is feasible that the bond is broken *in vivo*. In the reduced state, the thiol of GSH would be in hydrogen-bonding distance of Ser9, Cys10 or His106. Mutagenesis studies have shown that replacement of Ser9 by an alanine residue causes a 25% decrease in activity whereas replacement by a threonine residue caused a 2.5-fold increase in activity [37]. There was no observed shift in the apparent pK_a of bound GSH, however, unlike the shifts observed for mutations of the catalytic tyrosine or serine in other GST classes. Mutation of Cys10 in either the *P. mirabilis* or *E. coli* GSTs has no effect on conjugating activity [12,37]. The small but significant changes for Ser9 indicate that it has a contributory role in catalysis but suggest that His106 might have the major role in stabilizing the thiolate ion of GSH in the catalytic cycle of a conjugating reaction. Of the two candidate residues, only His106 is conserved in all the bacterial GSTs listed in the first grouping in Figure 7. The Nδ1 atom of His106 interacts with the hydroxyl group of Tyr157 and this interaction appears to orientate the Nε2 atom of His106 for optimal interaction with the thiolate GSH ion. Tyr157 is also strictly conserved in the listed bacterial GSTs suggesting that it has a critical role in catalysis by altering the pK_a of His106 and correctly orientating the latter residue for interaction with GSH. An alternative source of the stabilization that cannot be ruled out at this stage is the mainchain amide of Cys10, which is also within hydrogen-bonding distance of the thiolate ion.

The bacterial and closely related GSTs display minimal or no conjugating activity with standard GST substrates [16,17,19,38,39] and hence it is plausible that GSTs have different roles in bacteria from those in eukaryotes. A mechanism has recently been proposed for the reductive dehalogenation performed by tetrachlorohydroquinone dehalogenase, a member of the bacterial GST superfamily [20]. Mutagenesis studies have demonstrated that Cys13, the equivalent residue to Cys10 in PmGST B1-1 (see Figure 7), is directly involved in the reductive dehalogenation of tetrachlorohydroquinone. The first step in the postulated model is the attack of the thiolate anion of GSH onto the aromatic ring of the substrate, resulting in the displacement of a chloride ion. The GSH moiety is then displaced, with the aid of an acid and base, to form a mixed disulfide with Cys13. The wild-type protein is recovered, with another molecule of GSH breaking the mixed disulfide to form GSH disulfide. By analogy, the disulfide formed between GSH and Cys10 in PmGST B1-1 could represent the mixed disulfide intermediate in a similar reaction mechanism. Thus the role of PmGST B1-1 could be in the metabolic breakdown of aromatic compounds, like a number of other bacterial GSTs [19,20,39], rather then being a general detoxifier of foreign toxins.

The similarities in the fold of the N-terminal domain of GSTs with thioredoxin, glutaredoxin, glutathione peroxidase and the disulfide bond catalyzing enzyme DsbA have previously been noted (Figure 7b) [27–29]. Briefly, the βαβαββα motif of the N-terminal domain resembles the thioredoxin fold. Insertions of up to 70 residues have been observed in the same region where the extra β strand, β2a, has been inserted in the PmGST B1-1 structure (Figure 1a). Superpositions of the thioredoxin fold from each protein yield close structural matches with rms deviations on Cα atoms of between 1.7 Å and 2.8 Å [29]. In all but glutathione peroxidase, the *cis*-proline residue is conserved and superimposes at the same position in all structures. Beyond this residue, no sequence similarities have so far been identified running across the group. Of particular interest here is the common functional feature that all these proteins interact with substrates that possess either a thiol or disulfide group and form a mixed disulfide as part of their catalytic mechanism. Although the active-site cysteine regions of each protein do not superimpose, the substrate cysteine/cystine is positioned in the same relative location in space. Because of the very low activities of PmGST B1-1 with a range of GST substrates and the functional similarites with the thioredoxin superfamily, it is conceivable that the *in vivo* role of bacterial GSTs is as redox proteins rather than conjugating enzymes. In support of this, is the predominant localization of the enzyme to the periplasmic space [36], the low levels (0.6% of total cytosolic protein [25]) and the often highly specific activities of bacterial GSTs [19–22,39]. This is in contrast to other classes of GSTs that are widely distributed, present at high levels (3–5% of total cytosolic proteins) and display broad substrate specificity [1,2]. It has been proposed that a mixed disulfide between substrate thiol and a catalytic cysteine residue occurs in thioredoxin (for a review, see [40]). By analogy, the observation of a mixed disulfide in the PMGST B1-1 structure could represent an intermediate complex.

A new class of GSTs

PmGST B1-1 was originally classified as a theta class GST on the basis of very limited sequence similarity between

Figure 7

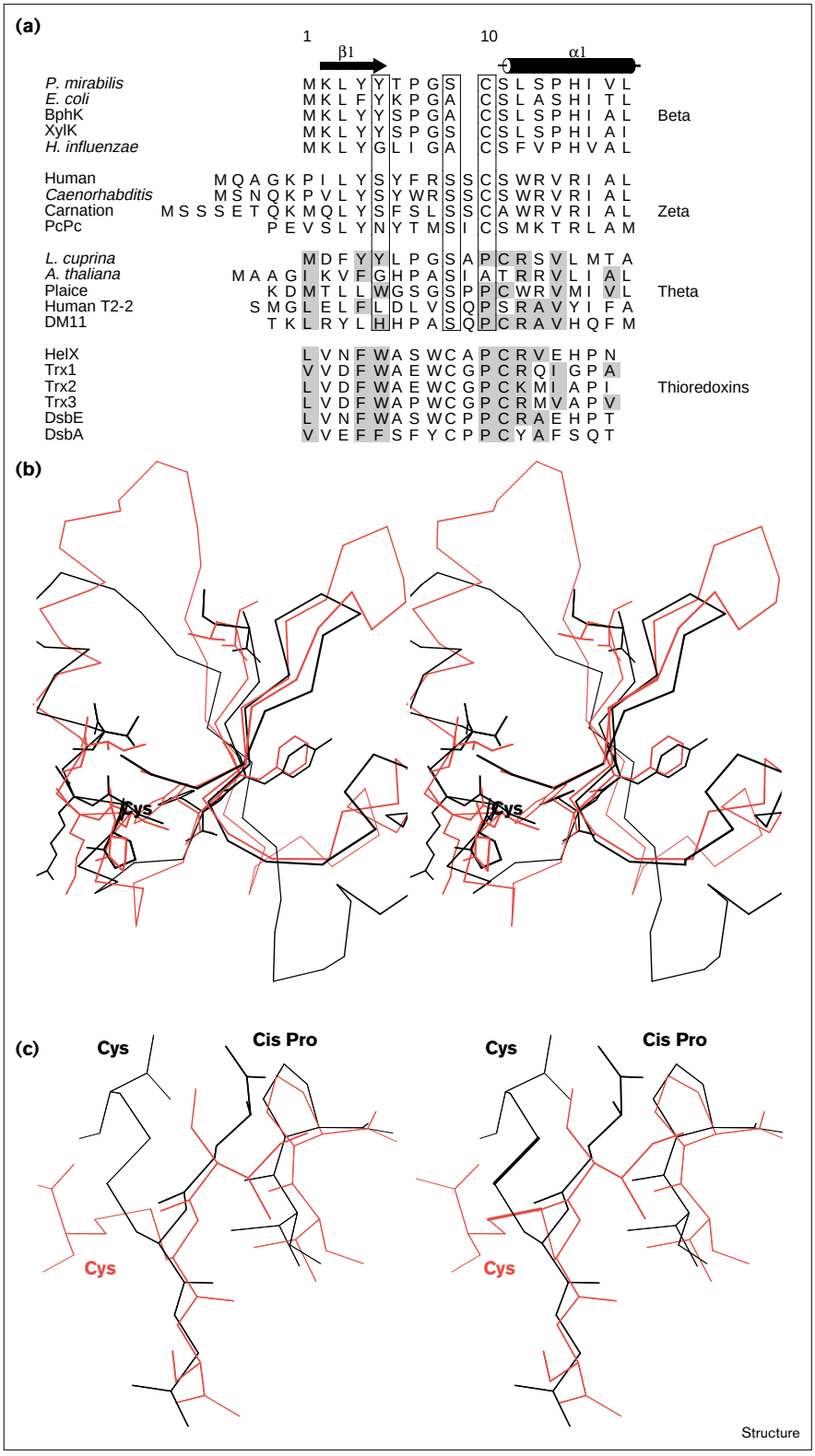

Evolutionary comparisons. **(a)** N-terminal sequence alignment of members from the beta, zeta and theta class GST families and of members from the thioredoxin superfamily. The sequences were aligned with AMPS and displayed using ALSCRIPT [58]. Where possible, alignments were based on three-dimensional structural superpositions as described below. The position of the catalytic tyrosine of the alpha, mu, pi and sigma class GSTs, the catalytic serine of the theta class GSTs and the cysteine residue found covalently bound to substrate in the beta class GSTs are all shown boxed. Shaded residues indicate strictly conserved or conservatively substituted residues that occur in at least two of both the theta and thioredoxin groupings. The secondary structure of PmGST B1-1 is shown above the alignment (defined using PROMOTIF [59]); numbering is according to the PmGST B1-1 sequence. Sequences are as follows (SWISSPROT OR GENBANK accession numbers are in parentheses): *P. mirabilis*, *Proteus mirabilis* GST B1-1 (GT_PROM1); *E. coli*, *Escherichia coli* GST (GT_ECOLI); BphK, protein from *Burkholderia* sp. strain LB400; XylK, protein from *Cycloclasticus oligotrophus*; *H. influenzae*, an open reading frame HI0111 from *Haemophilus influenzae*; Human, human zeta class GST (U86529); *Caenorhabditis*, *Caenorhabditis elegans* zeta class GST (Z66560); Carnation, an ethylene-responsive flower senescence-related enzyme from carnation (GTT1_DIACA); PcPc, tetrachloro-*p*-hydroquinone reductive dehalogenase from *Sphingomonas chlorophenolica* (PCPC_FLAS3); *L. cuprina*, blowfly GST (GTT1_LUCCU); *A. thaliana*, a plant GST (P46422); Plaice, fish GST (GT_PLEPL); Human T2-2, human theta class GST T2-2 (GTT2_HUMAN); DM11, dichloromethane dehalogenase (DCMA_METS1); HelX, a thioredoxin-like protein from *Rhodobacter capsulatus* (HELX_RHOCA); Trx1, thioredoxin from *Rhodobacter sphaeroides* (THIO_RHOSH); Trx2, thioredoxin from *E. coli* (THIO_ECOLI); Trx3, thioredoxin from *Anacystis nidulans* (THI1_ANANI); DsbE, a DsbE homolog from *Paracoccus denitrificans* (CCMG_PARDE); DsbA, a DsbA homolog from *Salmonella typhimurium*. **(b)** Comparison of *E. coli* thioredoxin (red trace) [43] and insect theta class GST (black trace) [13]. The superposition, performed with LSQMAN [60], was based on the Cα atoms of the common β strands. The sidechains of residues found conserved in the shared sequence motif are shown. **(c)** Comparison of human thioredoxin complexed to a peptide of Ref-1 (red trace) (PDB code 1CQH) [44] and PmGST B1-1 complexed to GSH (black trace). The restrained energy-minimized average structure of thioredoxin was superimposed onto PmGST B1-1 with LSQMAN [60] using the Cα atoms of the common β strands as a reference. The Ref1 peptide is covalently bound by its thiol to Cys32 and GSH is covalently bound to Cys10. (Figures b and c were produced using MOLSCRIPT [56].)

the N-terminal domain and mammalian theta class enzymes, despite displaying minimal or no detectable activity towards a range of standard GST substrates [23]. A number of workers have suggested that the theta class may require further division because of the widely divergent properties of some of its members [12,33]. PmGST B1-1 seems to belong to a new class of GSTs as it neither utilizes the catalytic tyrosine residue of the alpha, mu, pi and sigma class GSTs nor the catalytic serine residue of the theta class enzymes. We propose that PmGST B1-1 is the prototype for a new GST class which we call beta ('b' for bacterial). We have also included in this class a number of other bacterial GSTs that were previously classified as theta class GSTs (Figure 7a). The sequence identities between each family member are significant, ranging from 32% to 54%, and they all cluster together in dendograms [7,9,39]. All of these enzymes contain the two residues identified in the PmGST B1-1 structure as likely to be involved in the catalytic cycle: Cys10 and His106. As well as these residues, the sequence alignment about Cys10 is strongly conserved, with a serine and a large hydrophobic residue immediately following the cysteine. The crystal structure suggests that these two residues have structural roles.

Interestingly, not all bacterial GSTs fall into the beta class category (Figure 7a). For example, although dichloromethane dehalogenase has a cysteine residue adjacent to the position of Cys10 of PmGST B1-1 in the sequence alignment, it also has the conserved theta class serine. In this case, mutagenesis studies have clearly demonstrated that the serine residue is essential for catalytic activity [41]. Similarly, in the human and insect theta class enzymes, mutagenesis studies have shown this serine to be essential [14,15]. The sequence motif about the equivalent of the Cys10 position in the theta class enzymes is clearly different from that found in the beta class, where there is a one residue deletion immediately before the cysteine (Figure 7a). Where there is a cysteine residue at position 11 in the theta class enzyme, it is always proceeded by a proline residue (Figure 7a and data not shown). In the insect theta class GST crystal structure [13] this proline residue is located at the tip of the loop, at the equivalent position to Cys10 in the PmGST B1-1 structure, and the cysteine residue at position 11 is buried in the core of the N-terminal domain (Figure 6b). Previous sequence and functional comparisons have indicated that dichloromethane dehalogenase is more closely related to eukaryotic members of the theta class than to other bacterial GSTs [41]. For example, a rat theta class GST displays catalytic activity towards dichloromethane [42] whereas PmGST B1-1 does not [26].

A new class of GSTs, the zeta class, has recently been proposed on the basis of phylogenetic arguments [7]. The zeta class has an N-terminal motif that is distinct but closely related to that of the beta class. Key differences include a one-residue insertion immediately preceding Cys10 and a conserved basic residue at position 13. The zeta class also have a conserved tyrosine residue adjacent to the position of the catalytic tyrosine of the alpha, mu, pi and sigma classes and the conserved catalytic serine residue of the theta class. It is not known which residue is used to stabilize the GSH thiolate in the zeta class, although model building suggests the serine residue as the most likely candidate [7]. The putative catalytic residue His106 and the other residues from the C-terminal domain that interact with GSH in the beta class GSTs are lost in the zeta class enzymes (data not shown).

The evolutionary link between the GST and thioredoxin superfamilies

The close three-dimensional structural similarity between the N-terminal domains of GSTs and the thioredoxin fold has been noted by a number of laboratories [27–29]. The only residue that seems to be conserved between the two families, however, is the structurally important *cis*-proline residue. Whether the two families are related by divergent or convergent evolution has been an open question. Until the present study, the potential importance of the cysteine residue near the N terminus of some GSTs was overlooked as, unlike the catalytic tyrosine or serine residues, it did not seem to be well conserved across GSTs. The finding that Cys10 forms a mixed disulfide in the PmGST B1-1 crystal structure and the new beta class classification, highlighting the potential importance of the cysteine, prompted us to revisit this evolutionary question.

Although *E. coli* and human thioredoxins exhibit low pairwise sequence identity (25%), the active-site Trp-Cys-Gly-Pro-Cys motif is strictly conserved [40]. This motif has a striking similarity to the active-site consensus motif Hyd-Ser-Xxx-Pro-Cys (where Hyd is a hydrophobic residue and Xxx is any residue), found in many of the theta class enzymes (Figure 7a and data not shown). Indeed, it has already been remarked that whenever there is a cysteine residue at position 11 in the theta class alignment, a proline residue always precedes it. Structural superposition of the insect theta GST crystal structure [13] with the *E. coli* thioredoxin crystal structure [43] shows that the Pro-Cys of each superimpose exactly (Figure 7b). Further analysis shows that the consensus motif, [FYL][FYWHL]XXX[CS]XPC-[RKW]XV (where the square brackets denote positions that can be occupied by only one of the residues shown within the brackets), when scanned against the SWISSPROT sequence database, only detects either thioredoxin or theta class GST molecules. This is the first time that sequence similarities between the two superfamilies have been detected. In addition, the thioredoxin and GST families share the characteristic features of a peptide-binding groove (the G site) and a large, exposed hydrophobic region (the H site) surrounding their respective active sites. The

structure of human thioredoxin complexed to a peptide from the redox protein Ref-1 has been published [44]. We have superimposed this structure on the structure of PmGST B1-1 complexed to GSH (Figure 7c). There is a striking superposition of the Ref-1 peptide with the peptide backbone of GSH (Figure 7c). There is an antiparallel β-sheet-like interaction between the backbone of either peptide and the backbone of the residue preceding the *cis*-proline residue of each protein. Such an interaction has been observed in all GST–GSH complexes to date [10–12] and has also been observed in the complex of glutaredoxin and GSH [45]. It should be noted that peptides can bind in both orientations to human thioredoxin [44,46]. Assuming an evolutionary relationship between GSTs and a member of the thioredoxin superfamily, it seems that GSTs have either lost the capability of binding peptides in more than one orientation or, more likely, have evolved from a distant member of the thioredoxin superfamily that never had this capability. These comparisons support the proposal that GSTs did evolve from a thioredoxin ancestor and that the theta class represents the most ancient GST family.

The sequence alignments and dendograms [7,9,39] lead us to hypothesize an evolutionary pathway for GSTs. We suggest that the beta class GST evolved from an ancient theta class GST because of its wide distribution in a number of bacterial species. The polar subunit and domain interfaces in the beta class could be a relic of the monomeric thioredoxin-like molecule from which the ancient theta class enzymes evolved. The zeta class evolved from the beta class and spread out into more complex organisms. Modeling of the human zeta class enzyme suggests that the dimer interface might be more hydrophobic. We suspect that the one-residue insertion preceding residue 10 in the zeta class (Figure 7a) ensured that Cys10 could no longer form a disulfide with GSH and thus lifted the restrictive environment required for beta class activity. Because both the beta and zeta class GSTs exhibit very low or no activity towards standard GST substrates, quite often exhibit highly specific activities, and are present at much lower levels in cells compared with their mammalian counterparts, we suggest that the beta and zeta class GSTs were recruited for highly specialized metabolic roles in bacteria and represent an independent branch of GST evolution. The other classes also evolved from the ancestral theta class enzyme with the adaption of the lock-and-key pocket, the predominantly hydrophobic domain and subunit interfaces, and utilization of a tyrosine residue (alpha, mu, pi, sigma classes) in the catalytic mechanism. Figure 6 shows how the key catalytic residues developed during evolution. Of particular interest is the presence of the catalytic tyrosine in all three GSTs and its recruitment in the alpha, mu, sigma and pi enzymes caused by a twisting of β strand 1 to bring the sidechain into the active site, whereas any trace of the catalytic serine has been lost in these enzymes.

Biological implications

Glutathione *S*-transferases (GSTs) are found in a wide variety of organisms, ranging from bacteria to plants and animals. These enzymes detoxify a broad range of toxic compounds by catalyzing the conjugation of glutathione (GSH) onto the toxins. The activity of GSTs is believed to be a factor in the development of cellular resistance to antibiotics, herbicides, insecticides and clinical drugs and hence they are the subject of intense study.

Relatively little is known about bacterial GSTs because they exhibit limited conjugating activity with standard GST substrates and hence their existence in bacteria has been overlooked until recently. However, their subcellular distribution and often quite highly specific activities towards a narrow range of substrates suggests they have different roles in bacteria. This is the first report of a bacterial GST structure. *Proteus mirabilis* GST (PmGST B1-1) shares less than 20% sequence identity with the other GST classes yet adopts a similar three-dimensional fold. The N-terminal domain binds GSH in a mode of binding similar to that observed in other GST classes. In PmGST B1-1, however, a cysteine residue is found covalently bound to the substrate GSH. The finding of this mixed disulfide bond indicates that the catalytic mechanism of this enzyme must either be very different from that proposed previously for GSTs from other organisms, or that the enzyme functions differently in bacteria. These observations have led to the proposal that PmGST B1-1 belongs to a new class of GSTs we term beta. The beta class includes a number of other bacterial GSTs previously described as belonging to the theta class. The reclassification has led to the discovery of additional data which support the view that GSTs evolved from an ancestral member of the thioredoxin superfamily.

Materials and methods

Crystallization and data collection

Crystal form II was grown as previously described [47]. Briefly, crystals were obtained using 5 mg/ml of protein solution (made up in double-distilled water) with 22% to 28% PEG 8K as precipitant, 100 mM HEPES buffer (pH 6.5–7.3) and in the presence of 10 mM reduced GSH. The crystals grew at room temperature as long rods. The data collection statistics are given in Table 1. These crystals were difficult to reproduce and a structure determination based on diffraction data from them proved elusive.

Recently, a new crystal form, crystal form I, was obtained using the hanging drop vapour diffusion method. Crystals were obtained with 3–4 mg/ml protein solution (made up in double-distilled water) using 20% PEG 6K as precipitant, 100 mM citrate buffer (pH 4.6) and in the presence of 10 mM reduced GSH. The crystals were grown at room temperature. The bipyramid-shaped crystals belong to the space group $P4_122$ (or its enantiomorph $P4_322$) as judged by the data processing programs DENZO and SCALEPACK [48]. A monomer in the asymmetric unit corresponds to a V_m value of 2.4 Å^3/Da, which is within the range reported by Matthews [49]. The data collection statistics are presented in Table 1.

Structure determination

The structure was solved using the molecular replacement technique on the crystal form I data set. All molecular replacement studies were

Table 1

Summary of data collection statistics.

	I	II
Space group	$P4_122$	$P4_3$
Cell dimensions		
a (Å)	57.2	90.9
b (Å)	57.2	90.9
c (Å)	129.4	117.3
Temperature (K)	288	295
Detector*	MAR	HM (X-11)
Maximum resolution (Å)	2.5	2.7
Total no. of observations	31,800	60,878
No. of unique reflections	7618	22,464
Completeness of data (%)	95.0 (95.7)	85.8 (90.0)
Data $>2\sigma_I$ (%)	77.0 (57.2)	67.7 (52.5)
I/σ_I	17.0 (4.0)	7.8 (3.1)
Multiplicity	4.1	2.7
R_{merge} (%)†	8.0 (32.9)	14.7 (38.2)

*MAR is an in-house MAR research area detector and HM is the EMBL Outstation, DESY, Hamburg, Germany. The beamline used is shown in parentheses. †$R_{merge} = \Sigma_{hkl}\Sigma_i|I_i - \langle I\rangle|/|\langle I\rangle|$, where I_i is the intensity for the *i*th measurement of an equivalent reflection with indices *h,k,l*. The values in parentheses are for the highest resolution shell (approximate interval of 0.1 Å).

Table 2

Refinement statistics.

	I	II
Non-hydrogen atoms		
protein	1592	6368
substrate	40	160
water	52	0
Resolution (Å)	20.0–2.5	20.0–2.7
R_{factor} (%)*	20.2	21.5
R_{free} (%)†	30.1	24.5
Rmsd from ideal geometry		
bonds (Å)	0.007	0.007
angles (°)	1.2	1.3
dihedrals (°)	26.4	25.9
impropers (°)	0.7	0.7
Residues in most favoured regions of Ramachandran plot (%)	91.0	94.1

*$R_{factor} = \Sigma_{hkl}||F_{obs}|-|F_{calc}||/|F_{obs}|$, where F_{obs} denotes the observed structure-factor amplitude and F_{calc} denotes the structure-factor amplitude calculated from the model. †10% and 5% of reflections were used to calculate R_{free} for crystal forms I and II, respectively.

performed using the X-PLOR package [50]. The search model was the insect theta class GST from *Lucilia cuprina* [13]. The model was first converted to polyalanine and all loops removed as the level of sequence similarity (20%) between the insect and bacterial enzyme was low. Interestingly, although this crystal form contained only one monomer in the asymmetric unit, a successful molecular replacement solution could only be obtained when the dimer was used as a search model. The rotation function was calculated in the resolution range 12.0–5.5 Å (with a 2σ cut-off) and a Patterson radius of 28 Å. The correct solution was the highest peak. The Patterson correlation (PC) refinement protocol [51] was implemented as GSTs have shown variability in the intersubunit and interdomain angles. Using the top peak from the PC refinement (height of 0.18 whereas the next highest peak was 0.13), the translation function was used to resolve the space group ambiguity. In $P4_122$, this peak gave a top solution in the translation function (height of 0.39 whereas the next highest peak was 0.37). In $P4_322$, the top solution of the translation function (height of 0.35) was weaker, indicating that $P4_122$ was the correct enantiomorph. The correct solution placed the model close to a crystallographic twofold axis so that the biological dimer was created by the symmetry element. The preliminary pruned model packed well within the unit cell with no obvious symmetry clashes and an initial $2F_o-F_c$ electron-density map generated after rigid-body refinement was encouraging.

Model building and refinement

The structure was carefully built using a bootstrapping procedure involving multiple model building rounds interspersed with model refinement using either X-PLOR [50] or REFMAC [52]. A bulk-solvent correction was applied to the data and no sigma or low-resolution cut-offs were used to truncate the data. Restrained individual B factors were refined in the latter stages of refinement and this was accompanied by a significant drop in the R_{free} value. The R_{factor} was 56.0% and R_{free} was 54.0% for the starting model, which dropped to 20.2% and 30.1%, respectively, after 30 rounds of refinement. The substrate, GSH, was not built into the electron-density map until the last few cycles of refinement. Throughout the model-building steps, a strong continuous piece of density was always observed between Cys10 and the GSH thiol. Simulated annealing omit maps of the region supported the presence of a covalent bond between them (see Figure 3 and below). The final model accounts for all residues (1–201) except for the last two residues at the C terminus, one GSH molecule and 52 solvent molecules. The final map is of good quality (Figure 3) and good stereochemistry (Table 2). The stereochemical quality of the final model as assessed by PROCHECK [53] was excellent, with only two non-glycine residues (Glu65 and Lys87) in the generously allowed region of the Ramachandran plot whereas the rest were located in the most favored regions. Glu65, or its equivalent, has been found to be in a strained stereochemistry in all GST structures to date and is involved in GSH binding. Lys87 is located in the interdomain flexible linker and the density for this residue is not good enough to be certain of its stereochemistry. No residues scored below 0.1 in the 3D–1D profile, indicating that no residues were in chemically unreasonable environments [54]. There are five buried charge groups: Asp155 hydrogen bonds onto the mainchain amide of Thr152 and to the hydroxyl of Tyr181; Lys49 salt links onto Glu65; Asp75 salt links to Arg91; Glu104 salt links to Lys107 and Lys132; and Glu198 interacts with the mainchain of Gly8 and the sidechain of His15.

Crystal form II

This crystal form was solved by molecular replacement with AMoRe [55] using the final refined dimeric model from crystal form I (minus GSH and water molecules). The rotation function was calculated in the resolution range 10.0–4.0 Å and a Patterson radius of 28 Å. The correct solutions were the two highest peaks, both 7.4σ in height. The translation function indicated that the correct space group was $P4_3$. After rigid-body fitting in AMoRe, the correlation coefficient was 0.76 and the R_{factor} was 30.4%. Two rounds of positional refinement, with strict noncrystallographic symmetry restraints between the four monomers in the asymmetric unit and bulk-solvent correction yielded a model with R_{factor} of 21.5% (R_{free} of 24.5%) for all reflections to 2.7 Å resolution. Individual noncrystallographic symmetry-restrained B factors were refined in the last round of refinement (with tight restraints) and this was accompanied by a significant drop in the R_{free} value. The GSH molecule was included in the last few steps of refinement. To further test the presence of a disulfide between Cys10 and the GSH thiol, a refinement was performed assuming two free sulfhydryl groups and no restraints between them. The resultant electron-density map showed continuous strong density between the sulfur atoms even though the thiol groups of the model were now sitting out of density. The refinement was then repeated assuming a covalent connection. The distance between the sulfur atoms in the final model is 2.06 Å. The χ_3 angle of 156° indicates the disulfide is in a

strained conformation. The four monomers are identical with rms deviations for all Cα atoms of 0.01 Å. Only Glu65 lies outside the most favored region of the Ramachandran plot.

Accession numbers

The atomic coordinates have been submitted to the Brookhaven Protein Data Bank (accession codes 1PMT and 2PMT).

Acknowledgements

We thank Matthew Wilce for his work on the early stages of this project and the staff of the EMBL Outstation, DESY synchrotron, Hamburg, Germany for help with data collection. Financial support from the Australian Synchrotron Research Program for our visits to Hamburg is gratefully acknowledged. This Program is funded by the Commonwealth of Australia via the Major National Research Facilities Program. We thank Peter Reinemer for providing us with the plant GST coordinates. MWP is an Australian Research Council Senior Research Fellow and acknowledges project support from the Australian Research Council.

References

1. Mannervik, B. & Danielson, U.H. (1988). Glutathione transferases: structure and catalytic activity. *CRC Crit. Rev. Biochem.* **23**, 283-337.
2. Hayes, J.D. & Pulford, D.J. (1995). The glutathione S-transferase supergene family: regulation of GST and the contribution of the isoenzymes to cancer chemoprotection and drug resistance. *Crit. Rev. Biochem. Mol. Biol.* **30**, 445-600.
3. Mannervik, B., *et al*., & Jörnvall, H. (1985). Identification of three classes of cytosolic glutathione S-transferases common to several mammalian species: correlation between structural data and enzymatic properties. *Proc. Natl Acad. Sci. USA* **82**, 7202-7206.
4. Meyer, D.J., Coles, B., Pemble, S.E., Gilmore, K.S., Fraser, G.M. & Ketterer, B. (1991). Theta, a new class of glutathione transferase purified from rat and man. *Biochem. J.* **274**, 409-414.
5. Meyer, D.J. & Thomas, M. (1995). Characterization of rat spleen prostaglandin H D-isomerase as a sigma-class GSH transferase. *Biochem. J.* **311**, 739-742.
6. Pemble, S.E., Wardle, A.F. & Taylor, J.B. (1996). Glutathione S-transferase class kappa: characterisation by the cloning of the rat mitochondrial GST and identification of a human homologue. *Biochem. J.* **319**, 749-754.
7. Board, P.G., Baker, R.T., Chelvanayagam, G. & Jermiin, L.S. (1997). Zeta, a novel class of glutathione transferases in a range of species from plants to humans. *Biochem. J.* **328**, 929-935.
8. Pemble, S.E. & Taylor, J.B. (1992). An evolutionary perspective on glutathione transferases inferred from class-theta glutathione transferase cDNA sequences. *Biochem. J.* **287**, 957-963.
9. Buetler, T.M. & Eaton, D.L. (1992). Glutathione S-transferases: amino acid sequence comparison, classification and phylogenetic relationship. *Environ. Carcinogen. Ecotoxicol. Rev. C* **10**, 181-203.
10. Dirr, H.W., Reinemer, P. & Huber, R. (1994). X-ray crystal structures of cytosolic glutathione S-transferases. Implications for protein architecture, substrate recognition and catalytic function. *Eur. J. Biochem.* **220**, 645-661.
11. Wilce, M.C.J. & Parker, M.W. (1994). Structure and function of glutathione S-transferases. *Biochim. Biophys. Acta* **1205**, 1-18.
12. Armstrong, R.N. (1997). Structure, catalytic mechanism, and evolution of the glutathione transferases. *Chem. Res. Toxicol.* **10**, 2-18.
13. Wilce, M.C.J., Board, P.G., Feil, S.C. & Parker, M.W. (1995). Crystal structure of a theta-class glutathione transferase. *EMBO J.* **14**, 2133-2143.
14. Board, P.G., Coggan, M., Wilce, M.C.J. & Parker, M.W. (1995). Evidence for an essential serine residue in the active site of the theta class glutathione transferases. *Biochem. J.* **311**, 247-250.
15. Tan, K.-L., Chelvanayagam, G., Parker, M.W. & Board, P.G. (1996). Mutagenesis of the active site of the human theta-class glutathione transferase GSTT2-2: catalysis with different substrates involves different residues. *Biochem. J.* **319**, 315-321.
16. Di Ilio, C., *et al*., & Federici, G. (1988). Purification and characterization of three forms of glutathione transferase from *Proteus mirabilis. Biochem. J.* **255**, 971-975.
17. Iizuka, M., Inoue, Y., Murata, K. & Kimura, A. (1989). Purification and some properties of glutathione S-transferase from *Escherichia coli* B. *J. Bacteriol.* **171**, 6039-6042.
18. Arca, P., García, P., Hardisson, C. & Suárez, J.E. (1990). Purification and study of a bacterial glutathione S-transferase. *FEBS Lett.* **263**, 77-79.
19. La Roche, S.D. & Leisinger, T. (1990). Sequence analysis and expression of the bacterial dichloromethane dehalogenase structural gene member of the glutathione S-transferase supergene family. *J. Bacteriol.* **172**, 164-171.
20. McCarthy, D.L., Navarrete, S., Willett, W.S., Babbitt, P.C. & Copley, S.D. (1996). Exploration of the relationship between tetrachlorohydroquinone dehalogenase and the glutathione S-transferase superfamily. *Biochemistry* **35**, 14634-14642.
21. Toung, Y-P.S. & Tu, C-P.D. (1992). Drosophila glutathione S-transferases have sequence homology to the stringent starvation protein of *Eschericha coli. Biochem. Biophys. Res. Commun.* **182**, 355-360.
22. Masai, E., Katayama, Y., Kubota, S., Kawai, S., Yamasaki, M. & Morohoshi, N. (1993). A bacterial enzyme degrading the model lignin compound β-etherase is a member of the glutathione S-transferase superfamily. *FEBS Lett.* **323**, 135-140.
23. Mignogna, G., *et al*., & Martini, F. (1993). The amino acid sequence of glutathione transferase from *Proteus mirabilis,* a prototype of a new class of enzymes. *Eur. J. Biochem.* **211**, 421-425.
24. Hiratsuka, A., *et al*., & Sato, K. (1990). A new class of rat glutathione S-transferase Yrs-Yrs inactivating reactive sulfate esters as metabolites of carcingenic arylmethanols. *J. Biol. Chem.* **265**, 11973-11981.
25. Piccolomini, R., *et al*., & Federici, G. (1989). Glutathione transferase in bacteria: subunit composition and antigenic characterization. *J. Gen. Microbiol.* **135**, 3119-3125.
26. Perito, B., *et al*., & Di Ilio, C. (1996). Molecular cloning and overexpression of a glutathione transferase gene from *Proteus mirabilis. Biochem. J.* **318**, 157-162.
27. Reinemer, P., Dirr, H.W., Ladenstein, R., Schäffer, J., Gallay, O. & Huber, R. (1991). The three-dimensional structure of class pi glutathione S-transferase in complex with glutathione sulfonate at 2.3 Å resolution. *EMBO J.* **10**, 1997-2005.
28. Sinning, I., *et al*., & Jones, T.A. (1993). Structure determination and refinement of human alpha class glutathione transferase A1-1, and a comparison with the mu and pi class enzymes. *J. Mol. Biol.* **232**, 192-212.
29. Martin, J. (1995). Thioredoxin – a fold for all reasons. *Structure* **3**, 245-250.
30. Ji, X., Zhang, P., Armstrong, R.N. & Gilliland, G.L. (1992). The three-dimensional structure of a glutathione S-transferase from the mu class gene. Structural analysis of the binary complex of isoenzyme 3-3 and glutathione at 2.2 Å resolution. *Biochemistry* **31**, 10169-10184.
31. Reinemer, P., *et al*., & Parker, M.W. (1992). Three-dimensional structure of class pi glutathione S-transferase from human placenta in complex with S-hexylglutathione at 2.8 Å resolution. *J. Mol. Biol.* **227**, 214-226.
32. Ji, X., *et al*., & Gilliland, G.L. (1995). Three dimensional structure, catalytic properties, and evolution of a sigma class glutathione transferase from squid, a progenitor of the lens S-crystallins of cephalopods. *Biochemistry* **34**, 5317-5328.
33. Reinemer, P., *et al*., & Bieseler, B. (1996). Three-dimensional structure of glutathione S-transferase from *Arabidopsis thaliana* at 2.2 Å resolution: structural characterisation of herbicide-conjugating plant glutathione S-transferase and a novel active site architecture. *J. Mol. Biol.* **255**, 289-309.
34. Rossjohn, J., Board, P.G., Parker, M.W. & Wilce, M.C.J. (1996). A structurally derived consensus pattern for the theta class glutathione transferases. *Protein Eng.* **9**, 327-332.
35. McTigue, M.A., Williams, D.R. & Tainer, J.A. (1995). Crystal structures of a schistosomal drug and vaccine target: glutathione S-transferase from *Schistosoma japonica* and its complex with the leading antischistosomal drug praziquantel. *J. Mol. Biol.* **246**, 21-27.
36. Allocati, N., *et al*., & Di Ilio, C. (1994). Immunogold localization of glutathione transferase B1-1 in *Proteus mirabilis. FEBS Lett.* **354**, 191-194.
37. Casalone, E., *et al*., & Di Ilio, C. (1998). Site-directed mutagenesis of the *Proteus mirabilis* GST B1-1 glutathione-binding site. *FEBS Lett.,* in press.
38. Nishida, M., Kong, K-H., Inoue, H. & Takahashi, K. (1994). Molecular cloning and site-directed mutagenesis of glutathione S-transferase from *Eschericha coli. J. Biol. Chem.* **269**, 32536-32541.
39. Vuilleumier, S. (1997). Bacterial glutathione S-transferases: what are they good for? *J. Bacteriol.* **179**, 1431-1441.
40. Holmgren, A. (1995). Thioredoxin structure and mechanism: conformational changes on oxidation of the active-site sulfhydryls to a disulfide. *Structure* **3**, 239-243.
41. Vuilleumier, S. & Leisinger, T. (1996). Protein engineering studies of dichloromethane dehalogenase/glutathione S-transferase from *Methylophilus* sp. strain DM11. Ser 12 but not Tyr 6 is required for enzyme activity. *Eur. J. Biochem.* **239**, 410-417.

42. Blocki, F.A., Logan, M.S.P., Baoli, C. & Wackett, L.P. (1994). Reaction of rat liver glutathione S-transferases and bacterial dichloromethane dehalogenase with dihalomethanes. *J. Biol. Chem.* **269**, 8826-8830.
43. Holmgren, A., Söderberg, B.-O., Eklund, H. & Brändén, C.-I. (1975). Three-dimensional structure of *Escherichia coli* thioredoxin-S_2 to 2.7 Å resolution. *Proc. Natl Acad. Sci. USA* **72**, 2305-2309.
44. Qin, J., Clore, G.M., Kennedy, W.M.P., Kuszewski, J. & Gronenborn, A.M. (1995). The solution structure of human thioredoxin complexed with its target peptide from Ref-1 reveals peptide chain reversal. *Structure* **4**, 613-620.
45. Bushweller, J.H., Billeter, M., Holmgren, A. & Wüthrich, K. (1994). The nuclear magnetic resonance solution structure of the mixed disulfide between *Escherichia coli* glutaredoxin (C14S) and glutathione. *J. Mol. Biol.* **235**, 1585-1597.
46. Qin, J., Clore, G.M., Kennedy, W.M.P., Huth, J.R. & Gronenborn, A.M. (1995). Solution structure of human thioredoxin in a mixed disulfide intermediate complex with its target peptide from the transcription factor NFκB. *Structure* **3**, 289-297.
47. Feil, S.C., *et al*., & Parker, M.W. (1996). Crystallization and preliminary X-ray analysis of a bacterial glutathione transferase. *Acta Cryst. D* **52**, 189-191.
48. Otwinowski, Z. (1993). Oscillation data reduction program. In *Proceedings of the CCP4 Study Weekend: Data Collection and Processing.* (Sawyer, L., Isaacs, N. & Bailey, S., eds), pp. 56-62, SERC Daresbury Laboratory, Warrington, UK.
49. Matthews, B.W. (1968). Solvent content of protein crystals. *J. Mol. Biol.* **33**, 491-497.
50. Brünger, A.T. (1992). *X-PLOR, Version 3.1. A system for X-ray crystallography and NMR.* Yale University Press, New Haven, CT.
51. Brünger, A.T. (1990). Extension of molecular replacement: a new search strategy based on patterson correlation refinement. *Acta Cryst. A* **46**, 46-57.
52. Murshudov, G.N., Vagin, A.A. & Dodson, E.J. (1997). Refinement of macromolecular structures by the maximum-likelihood method. *Acta Cryst. D* **53**, 240-255.
53. Laskowski, R.A., MacArthur, M.W., Moss, D.S. & Thornton, J.M. (1993). PROCHECK: a program to check the stereochemical quality of protein structures. *J. Appl. Cryst.* **26**, 283-291.
54. Lüthy, R., Bowie, J.U. & Eisenberg, D. (1992). Assessment of protein models with 3-dimensional profiles. *Nature* **356**, 83-85.
55. Navaza, J. (1994). AMoRe: an automated package for molecular replacement. *Acta Cryst. A* **50**, 157-163.
56. Kraulis, P.J. (1991). MOLSCRIPT: a program to produce both detailed and schematic plots of proteins. *J. Appl. Cryst.* **24**, 946-950.
57. Wallace, A.W., Laskowski, R.A. & Thornton, J.M. (1995). LIGPLOT: a program to generate schematic diagrams of protein–ligand interactions. *Protein Eng.* **8**, 127-134.
58. Barton, G.J. (1993). ALSCRIPT – a tool to format multiple sequence alignments. *Protein Eng.* **6**, 37-40.
59. Hutchinson, E.G. & Thornton, J.M. (1996). PROMOTIF – A program to identify and analyze structural motifs in proteins. *Protein Sci.* **5**, 212-220.
60. Kleywegt, G. (1996). Use of non-crystallographic symmetry in protein structure refinement. *Acta Cryst. D* **52**, 842-857.